ROLE OF LATENT HEAT RELEASE IN EXTRATROPICAL CYCLONE DEVELOPMENT

Phillip J. Smith
Department of Earth and Atmospheric Sciences
Purdue University
West Lafayette, IN, USA

1. INTRODUCTION

The relationship between extratropical cyclone (ECY) systems and their associated clouds and precipitation has been a matter of long-standing interest in meteorology. The successful prediction of cloud/precipitation distributions and amounts depends significantly on proper anticipation of the location and intensity of precursor cyclone events. But, in addition, the latent heat that is released during water vapor phase changes feeds back to the cyclone system to influence the latter's mass distribution and circulation intensity. It is this relationship between latent heat release (LHR) and cyclone development that is the subject of this paper.

There is no doubt that LHR influences ECY development. However, questions still remain regarding the mechanisms by which LHR exerts this influence. Further, in recognition of the existence of other ECY forcing processes, we must also be curious about LHR's "relative" importance among these various competing influences.

Modern efforts to address these issues, dating from the mid-1950's, can be categorized in two groups. The most extensive is a collection of observational data studies (e.g., Aubert, 1957; Danard, 1964, 1966b; Krishnamurti, 1968; Bullock and Johnson, 1971; Vincent et al., 1977; Lin and Smith, 1979, 1982; Bosart, 1981; DiMego and Bosart, 1982; Gyakum, 1983a, b; Keyser and Johnson, 1984; Pagnotti and Bosart, 1984; Smith et al., 1984; Smith and Dare, 1986; Reed and Albright, 1986; Tsou et al., 1987). However, in more recent years a second group of studies has emerged which have explored the impact of moist processes using numerical model simulations (e.g., Danard, 1966a; Tracton, 1973; Anthes and Keyser, 1979; Chang et al., 1982, 1984; Anthes et al., 1982; Kenney and Smith, 1983; Chen

et al., 1983; Robertson and Smith, 1983; Dare and Smith, 1984).

Within these studies the range of diagnosed parameters has been great indeed. Papers describing increased upper-level temperatures (Anthes et al., 1982; Chen et al., 1983), increased upper-level and decreased lower-level isobaric heights (Aubert, 1957, Danard, 1966a, b; Robertson and Smith, 1983; Chang et al., 1982; Tsou et al., 1987) and lowered sea-level pressure (Anthes and Keyser, 1979; Anthes et al., 1982; Robertson and Smith, 1983; Chen et al., 1983) attest to the role that LHR can play in altering the basic structure of atmospheric systems. Others have noted increased upper-and lower-level circulations (Anthes et al., 1982; Chang et al., 1982; Chen et al., 1983), enhanced upward vertical motion (Aubert, 1957; Danard, 1964; Krishnamurti, 1968; DiMego and Bosart, 1982; Pagnotti and Bosart, 1984; Smith et al., 1984) and vorticity (Tracton, 1973; Chang et al., 1982; Chen et al., 1983) fields, and more vigorous energy cycles (Danard, 1964, 1966b; Chang et al., 1984; Kenney and Smith, 1983; Robertson and Smith, 1983; Smith and Dare, 1986).

The results presented in this paper utilize the second of the above two approaches. More specifically, we present diagnoses of evolving extra-tropical cyclones as simulated by numerical prediction models run in two modes, one with full moist physics present (moist) and one with moist physics removed (dry). The principle results are for two cyclone cases simulated by the National Meteorological Center's Limited-Area Fine Mesh Model (LFM). In these experiments we are not concerned with the accuracy of the forecast. Rather, we utilize the model fields as "simulated observational data" in order to study the sensitivity of cyclone evolution to LHR.

2. METHODOLOGY

a. Model characteristics

Results described in the next section begin with an examination of the changing central sea level pressures in moist and dry simulations of five ECY cases. Three of these were simulated using the Drexel University Limited Area Mesoscale Prediction System (LAMPS). This model is described by Perkey (1976), Perkey and Kreitzberg (1976), and Chang et al. (1981) and is briefly summarized in Robertson and Smith (1983). Thus, it is not discussed here. The other two cases were simulated using the LFM model.

Following this initial examination, a more in depth diagnosis of the latter two cases is presented. Thus, since the principle results are those derived from the LFM, a short review of the key properties of this model is in order. Descriptions of the LFM model can be found in Gerrity (1977) and Newell and Deaven (1981), although some modifications to the model have been made since 1981. The most crucial parameterizations for this study are those that prescribe large-scale and subgrid-scale precipitation. Large-scale or "stable" precipitation is related primarily to the grid-scale saturation surplus or deficit. If a saturation surplus exists in a layer, the excess is removed as precipitation, releasing a commensurate amount of latent heat in that layer. If, on the other hand, a saturation deficit occurs, any precipitation falling into that layer is evaporated until saturation is achieved, with evaporative cooling occurring as well. The calculation progresses downward from the highest layer containing moisture. Subgrid-scale or "convective" precipitation is assumed to occur if the following criteria are met:

1) grid-scale precipitable water is increasing with time, indicative of moisture convergence;
2) grid-scale moisture is greater than 75% of saturation;
3) lifted condensation level for the layer in question (layer k) is below the midpoint of the next layer above (layer k + 1); and
4) parcel temperature is warmer by more than 0.1°C than the layer temperature of the next layer above, after having been given an initial impulse of 1.5°C.

Convective precipitation (r_c) is then proportional to the difference between the parcel potential temperature (the potential temperature a parcel would attain if lifted first dry then moist adiabatically from the midpoint of layer k to the midpoint of layer k+1) and the environmental potential temperature. The amount of convective precipitation is the smaller of r_c and the precipitable water, with the latter being depleted by the amount of precipitation. The calculation proceeds from the boundary layer upwards with any released latent heat calculated for layer "k" being assigned to layer "k+1", to simulate upward convective transport of heat. No evaporation is allowed.

Gridded data fields used to initiate the simulations were provided by NMC using their standard analysis/initialization procedures. Forecast fields were processed using a post-processor developed at Purdue by John Shively.

The domain of post-processed data is depicted in Fig. 1. The Purdue post-processor interpolates the sigma-level fields to pressure levels in 50 mb increments from 1050 mb to 50 mb linearly in ln p using the same algorithm contained in the LFM post-processor. The greater vertical resolution of the pressure-level data was chosen to decrease vertical truncation error in subsequent diagnostic calculations as well as to preclude vertical interpolation error in the post-processing. However, it must be kept in mind that the inherent vertical resolution of the LFM fields is rather coarse (see Fig. 2). The post-processor also converts potential temperature to temperature and precipitable water to relative humidity, the latter of which is bounded by 10% and 100%, in each layer. The vertical motion in isobaric coordinates (ω) is calculated in the LFM on sigma surfaces as the total derivative of pressure and is interpolated in the post-processor to pressure surfaces.

In order to examine the impact of latent heating, the code was modified to allow model experiments with and without LHR. For the simulations without LHR, both the convective and stable precipitation routines in the model were bypassed and the relative humidity in the model was maintained everywhere at 10%. All quantities required for the diagnoses were output at 6 h intervals throughout the 48 h forecast period.

b. Diagnostic parameters

In addition to the central sea level pressures, the diagnoses utilize two other parameters, the total latent heat release and the height tendency. These latter parameters are presented as area averages over a 2300 km square box ($12\Delta x$ by $12\Delta y$) centered on and moving with the ECY, as shown in Fig. 3. There are referred to as "cyclone averages" and are identified with an overbar ($\overline{\ }$). The height tendencies are obtained from a form of the height tendency equation, used for two reasons. First, the height tendency is a simple field which contains easily recognizable signatures corresponding to development and propagation features of a wave system. Second, the height tendency diagnosis can be accomplished with an equation which permits a separate examination of the diabatic and adiabatic forcing, a partitioning which is advantageous for this study. The height tendency equation used in this study is one that was developed and discussed in a recent paper by Tsou et al. (1987). Identified as the extended height tendency equation, this form is a simplified version of a general height

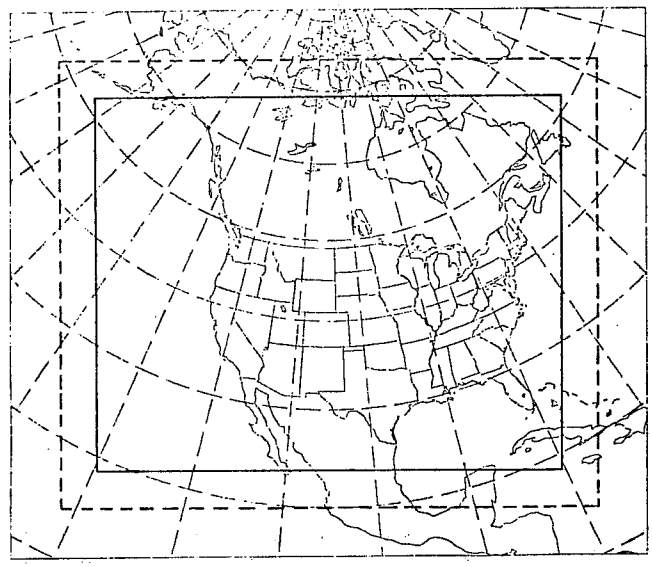

Fig. 1. LFM domain (outer boundary), post-processed data domain (dashed boundary), and computational domain (solid boundary).

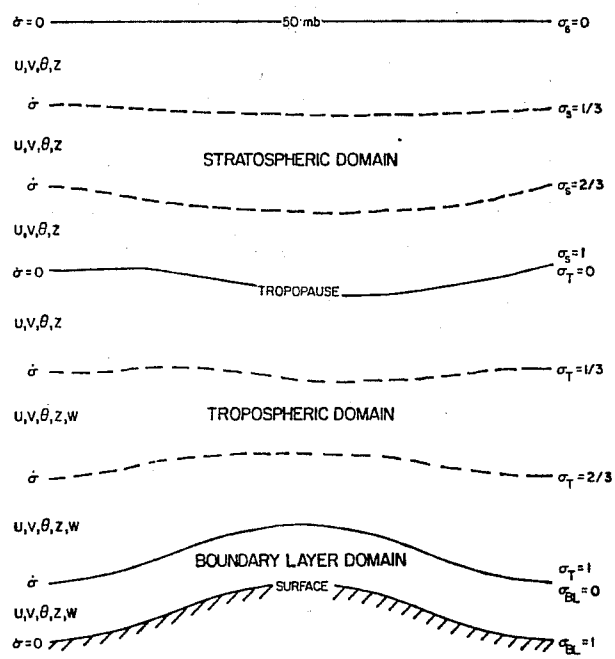

Fig. 2. Vertical structure of the LFM.

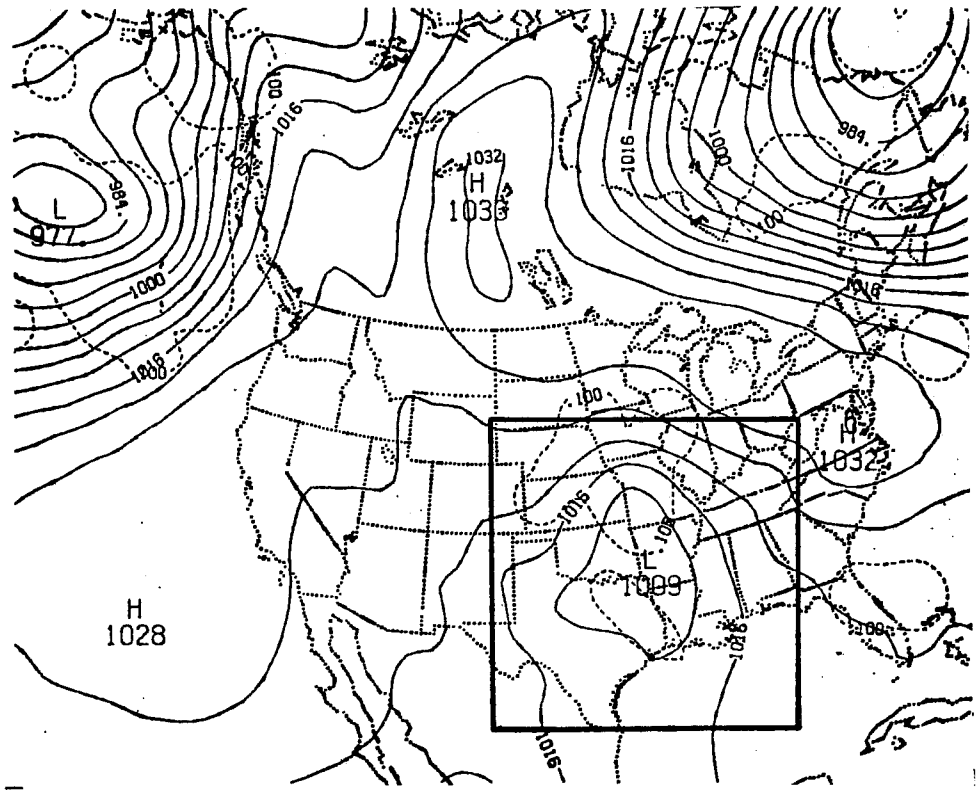

Fig. 3. Sample configuration of the cyclone averaging box.

tendency equation that can be derived by combining the general forms of the vorticity and thermodynamic equations. Following a scale analysis for Rossby numbers ranging from 0.1 to 0.5 and some sample calculations, the extended equation in a form appropriate for computation on the LFM grid becomes

$$m^2\left[\nabla^2 + \frac{(\zeta+f)f}{\sigma}\frac{\partial^2}{\partial p^2}\right]\frac{\partial\varphi}{\partial t} = -fm^2\frac{\vec{V}}{m}\cdot\nabla(\zeta+f) + \frac{(\zeta+f)f}{\sigma}m^2R\frac{\partial}{\partial p}\left(\frac{\vec{V}}{m}\cdot\nabla\frac{T}{p}\right)$$

(A) (B) (C)

$$- \frac{(\zeta+f)f}{\sigma}\frac{R}{c_p}\frac{\partial}{\partial p}\left(\frac{\dot{q}}{p}\right) - \frac{(\zeta+f)f}{\sigma}\omega\frac{\partial\sigma}{\partial p}, \qquad (1)$$

(D) (E)

where ζ is the relative vorticity, f the Coriolis parameter, T the temperature, σ the static stability parameter given by

$$\sigma = -\frac{RT}{p\Theta}\frac{\partial\Theta}{\partial p}, \qquad (2)$$

and Θ the potential temperature. Note that the height field (z) enters (1) through the defining relationship $\varphi = gz$, where $g = 9.8\ m\ s^{-2}$. Term A on the left-hand side of (1) is the LaPlacian of the height tendency, which can be shown to be proportional to the negative of the height tendency for wave-like solutions.

On the right-hand-side, term B (VORT) forces the height tendency by the horizontal advection of absolute vorticity. In quasigeostrophic theory, this term is considered to contribute primarily to the propagation of a wave system, since the geostrophic vorticity maximum (minimum) is generally centered in the base of the trough (ridge) and thus yields zero height tendencies in these locations (Holton, 1979, pp. 133-134). However, the actual vorticity may be asymmetric with respect to the trough and ridge, implying that in the extended form of the height tendency equation this term can contribute to the development of the wave as well as to its propagation.

Term C (THER) represents forcing by the vertically-differential horizontal thermal advection. It describes the contribution to the height tendency by the vertical gradient of the inverse-pressure-weighted temperature advection. The quasigeostrophic analog of this term is considered to be responsible for development of a wave system (Holton, 1979, pp. 134-135). In a typical developing extratropical system, the thermal and height fields are out of phase in the lower troposphere, become in phase in the upper troposphere, and yield cold-air advection in the trough and warm-air advection in the ridge that decrease with height. Obviously, significant contributions by this term are favored by the presence of baroclinicity.

The third forcing term in (1) is term D (HEAT), the vertically-differential heating term. It contributes to the height tendency through the vertical gradient of the inverse-pressure-weighted heating. Since LHR dominates the heating fields predicted by the LFM, this term yields a diagnosis of the direct influence of latent heating on the development of a wave system. Thus, this term attains significant values only in regions of LHR and typically produces height falls at levels below the maximum $\dot{q}$, height rises at upper levels, and little change at the level of maximum heating.

The fourth forcing term in the extended height tendency equation is the vertical advection of static stability, term E (STAB). An examination of (1) shows that this term is composed of three factors--a positive coefficient (seen also on the left-hand side and in terms C and D), the vertical motion, and the vertical derivative of static stability. Since static stability generally increases with decreasing pressure $\partial\sigma/\partial p$ is generally negative. Thus, the sign of the term and the sign of the height tendency for a wavelike solution are usually determined by the sign of the vertical motion, with upward advection of less stable air leading to height rises and downward advection of more stable air leading to height falls. The implication of this simple analysis is that the height tendencies due to term E generally oppose those due to terms B and C, yielding height rises ahead of the trough and height falls ahead of the ridge. The static stability parameter, σ, enters in the development of (1) through the thickness tendency equation, where it is coupled with vertical motion in the adiabatic heating/cooling term. σ specifies where vertical motions are most effective in producing thickness changes. In terms of the height tendency, however, it is not the static stability but the vertical

derivative of static stability that specifies the impact of vertical motions.

Note that (1) retains the basic simplicity of the more familiar quasi-geostrophic form (Holton, 1979, p. 131) but extends the latter by 1) utilizing model-generated (rather than geostrophic) winds, thus including ageostrophic effects; 2) permitting strong diabatic forcing; and 3) allowing three-dimensionally varying static stability.

The forcing terms on the right-hand side of (1) were calculated using the same fourth-order horizontal and second-order vertical centered finite-difference scheme used in the LFM. Calculations were performed on the computational domain indicated in Fig. 1 using simultaneous relaxation with zero boundary conditions ($\partial\varphi/\partial t = 0$) on all boundaries. The pressures of the upper and lower boundaries of the computational domain were set to 50 mb and the first level above the surface, respectively. Comparison of height changes derived from (1) with finite height changes obtained from the model predictions revealed performance of the extended height tendency equation comparable to that reported by Tsou et al. (1987).

3. MODEL SIMULATIONS

A variable often used to follow the changing intensity of an ECY is its central sea level pressure. Figs. 4 and 5 depict central pressure changes for five cyclone simulations over the United States; including three weak development cases (24 h $\Delta p \leq 6$ mb, Fig. 4), one strong development case (24 h $\Delta p > 10$ mb for both 24 h periods, Fig. 5), and one case which exhibited weak development during the first 24 h and strong development during the second 24 h (Fig. 5). The May 1977, January 1975, and October 1973 cases were simulated using the LAMPS model; the first two are described in Robertson and Smith (1983). The remaining two were simulated using the LFM model and will be discussed in more detail later. For additional comparison the 6 h positions of the simulated cyclone centers are shown in Fig. 6.

Comparison of Figs. 4 and 5 reveals an interesting contrast between strong and weak development cases. During periods of strong development (Fig. 5) a significant cyclone event evolves whether latent heat release is present or not, suggesting that moist processes may be important but are not

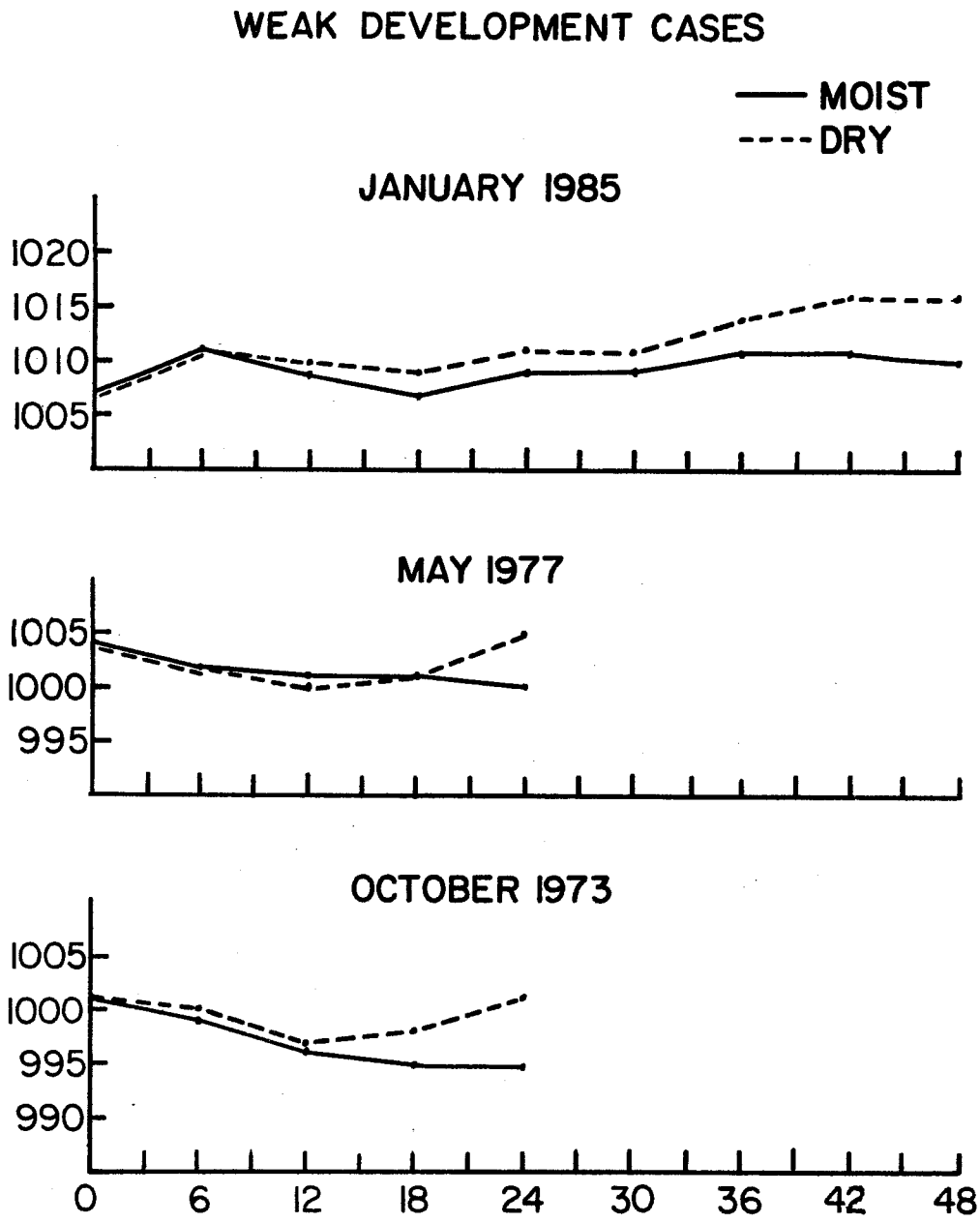

Fig. 4. Moist and dry simulated central sea level pressure for three weak development cases.

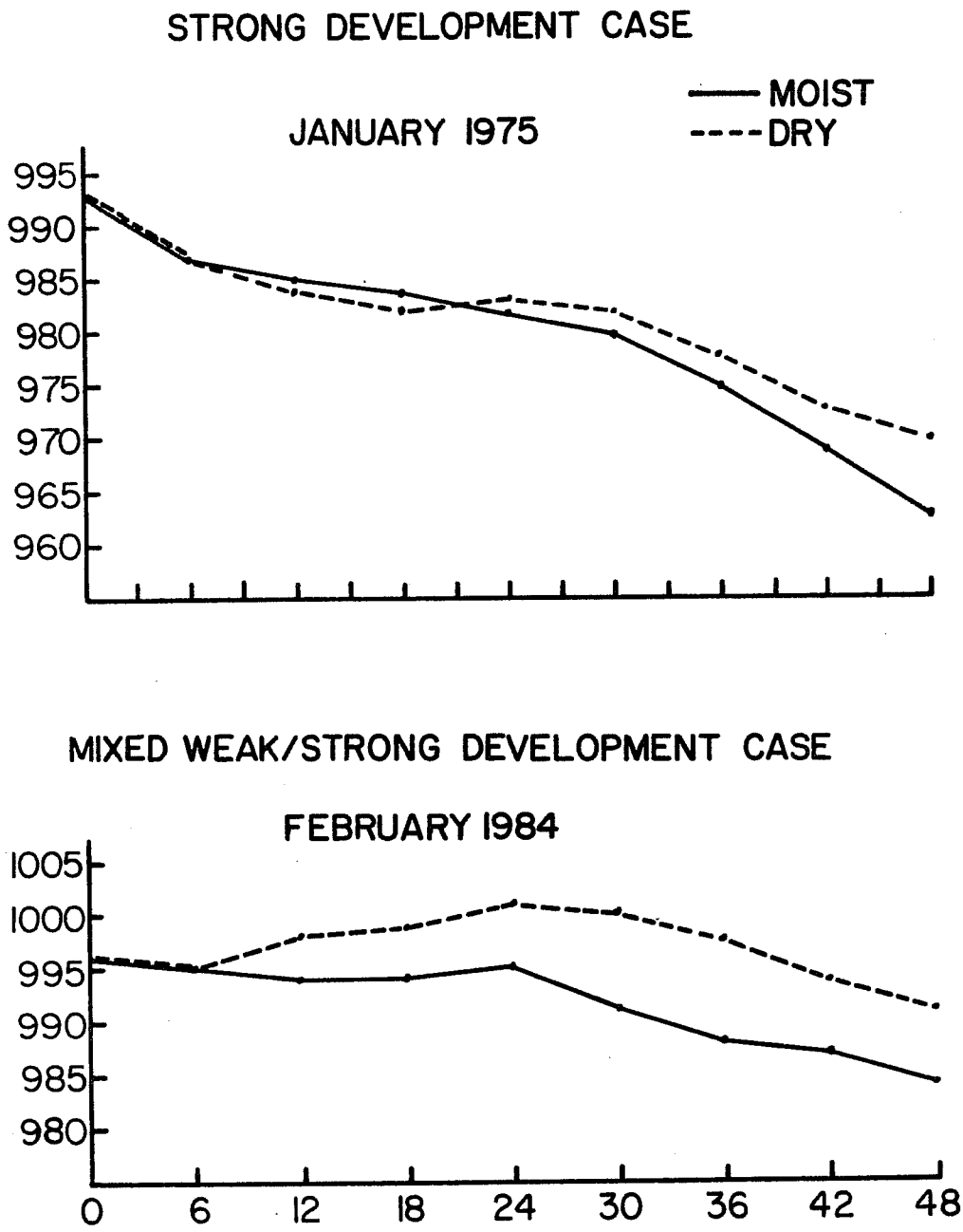

Fig. 5. As in Fig. 4 for one strong development and one mixed weak/strong development case.

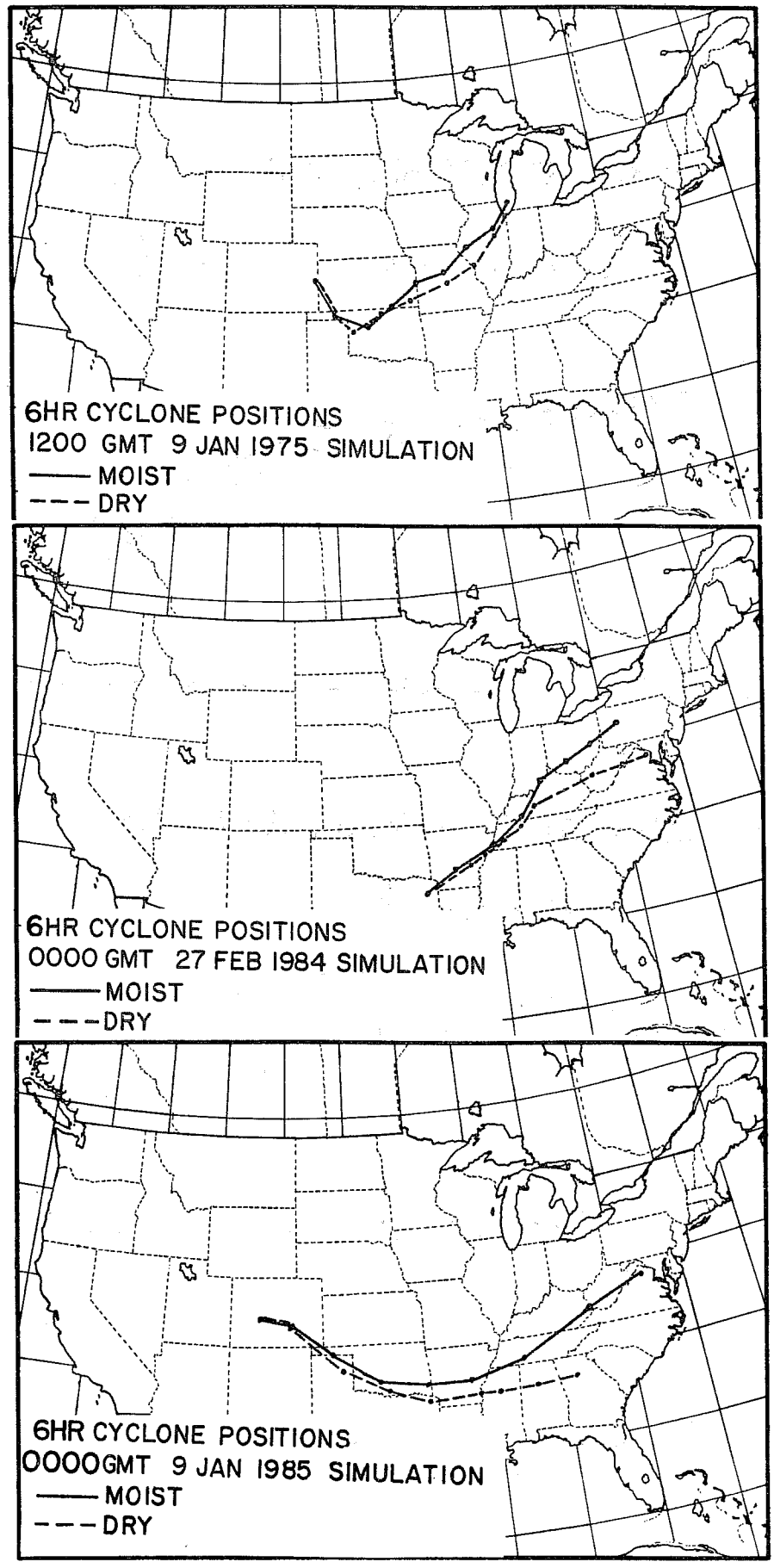

Fig. 6. 6 h positions of three simulated sea level cyclone centers.

crucial to cyclone development in such cases. In contrast, during weak development periods (Fig. 4, bottom of Fig. 5) the presence of latent heating is critical to the development, i.e., without latent heating the central pressure increases. Examination of Fig. 6 reveals that this relative importance during strong and weak development is also reflected in the cyclone propagation. While the "dry" cyclone tracks are generally south of the "moist" tracks, this distinction is much clearer for the weak case (January 1985) and the mixed weak/strong case (February 1984) than for the strong (January 1975).

To comment further on the relative importance of latent heating, the remaining discussion in this section and that in the next section will focus on the two LFM simulated cases, both represented by 48 h moist and dry simulations beginning at 0000 GMT 27 February 1984 (mixed weak/strong) and 0000 GMT 9 January 1985 (weak). The initial conditions for these cases are presented in Fig. 7. Of special interest is the cyclone over northeastern Texas on 27 February and the cyclone over central Colorado on 9 January. To conserve space, presentation of the simulations is restricted to the 48 h moist and dry fields in Figs. 8 and 9. In the February case the northeastward propagation and intensification of the system is apparent. In addition, one can see the greater extension of warm air north of the cyclone at 700 mb in the moist simulation and the cold air south of the cyclone in the dry, similar vertical motion patterns at 500 mb, and similar isotach structure at 300 mb. Analogous comparisons for the January case indicate that the relatively greater role of latent heating for this case is restricted to the lower troposphere.

Cyclone-area average LHR for the two moist simulations are presented in Fig. 10. Both cases yield maximum latent heating in the 550-600 mb layer. The more intense February case stimulates latent heating that is about three times larger and peaks about 12 h earlier than that of the January case.

4. HEIGHT TENDENCY RESULTS

To exemplify the height tendency distributions, attention is focused on the 48 h moist simulations. Figs. 11 and 12 depict 6 h equivalent 700 mb height changes simulated by the moist model for the two cases. In the February case, terms B, C, and D force height falls over and downstream

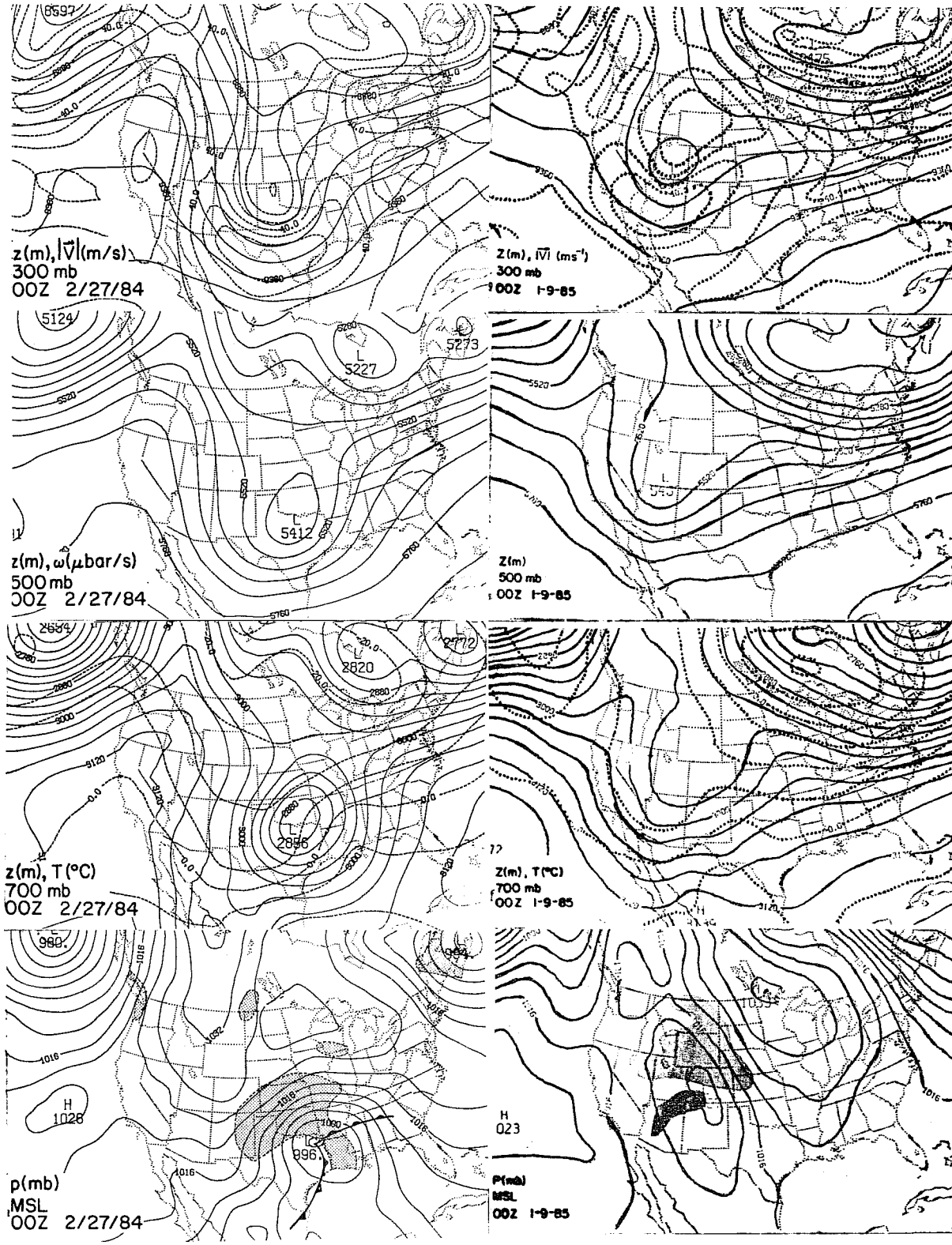

Fig. 7. Initial sea level pressure (mb) and precipitation shield (shaded), 700 mb height (m) and temperature (°C), 500 mb height (m), and 300 mb height (m) and wind speed (m s^{-1}) for the LFM February case (left) and January case (right).

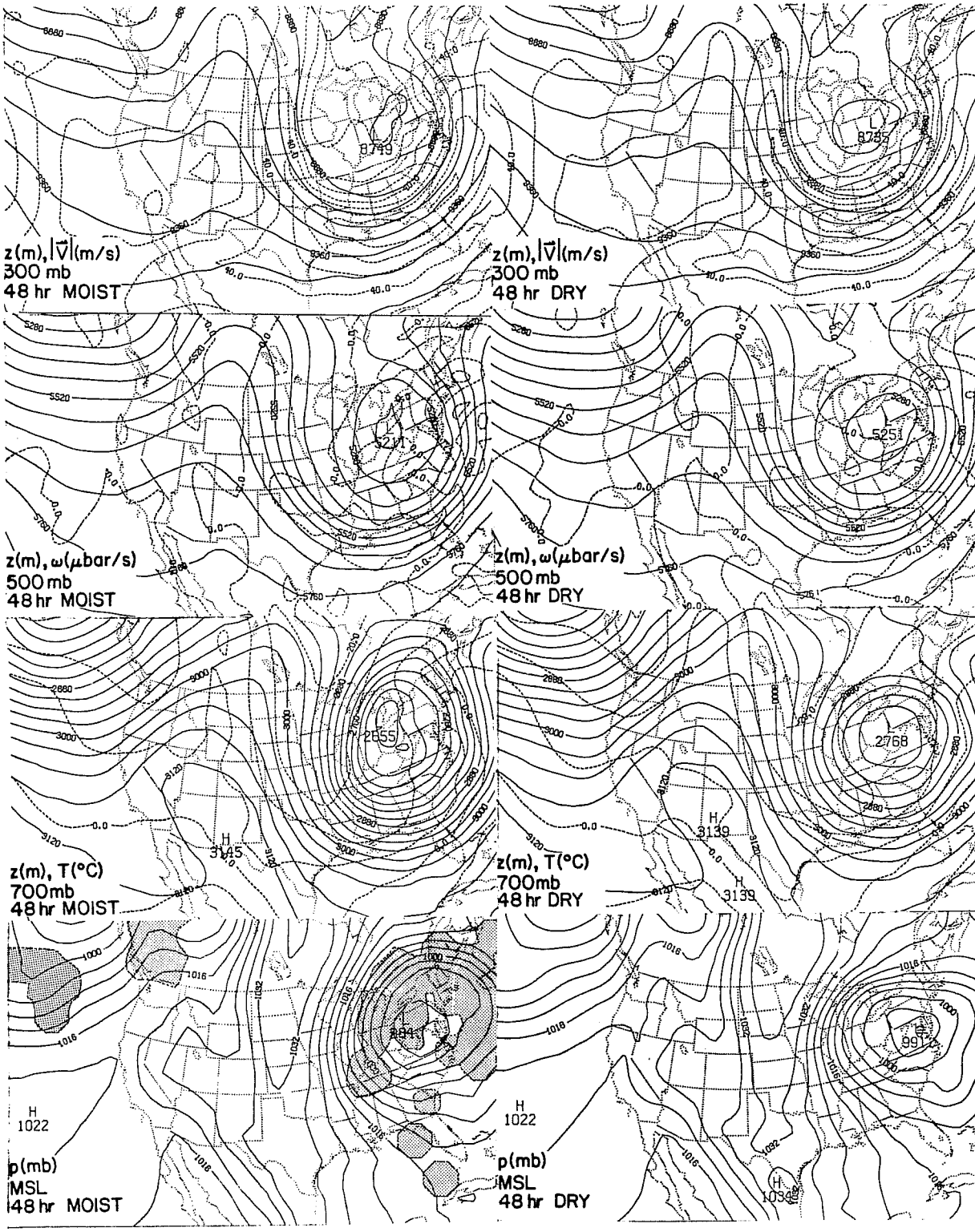

Fig. 8. 48 h moist and dry LFM simulations initialized at 0000 GMT 27 February 1984. Fields as in Fig. 7 with 500 mb vertical motions ($\mu bar\ s^{-1}$) added.

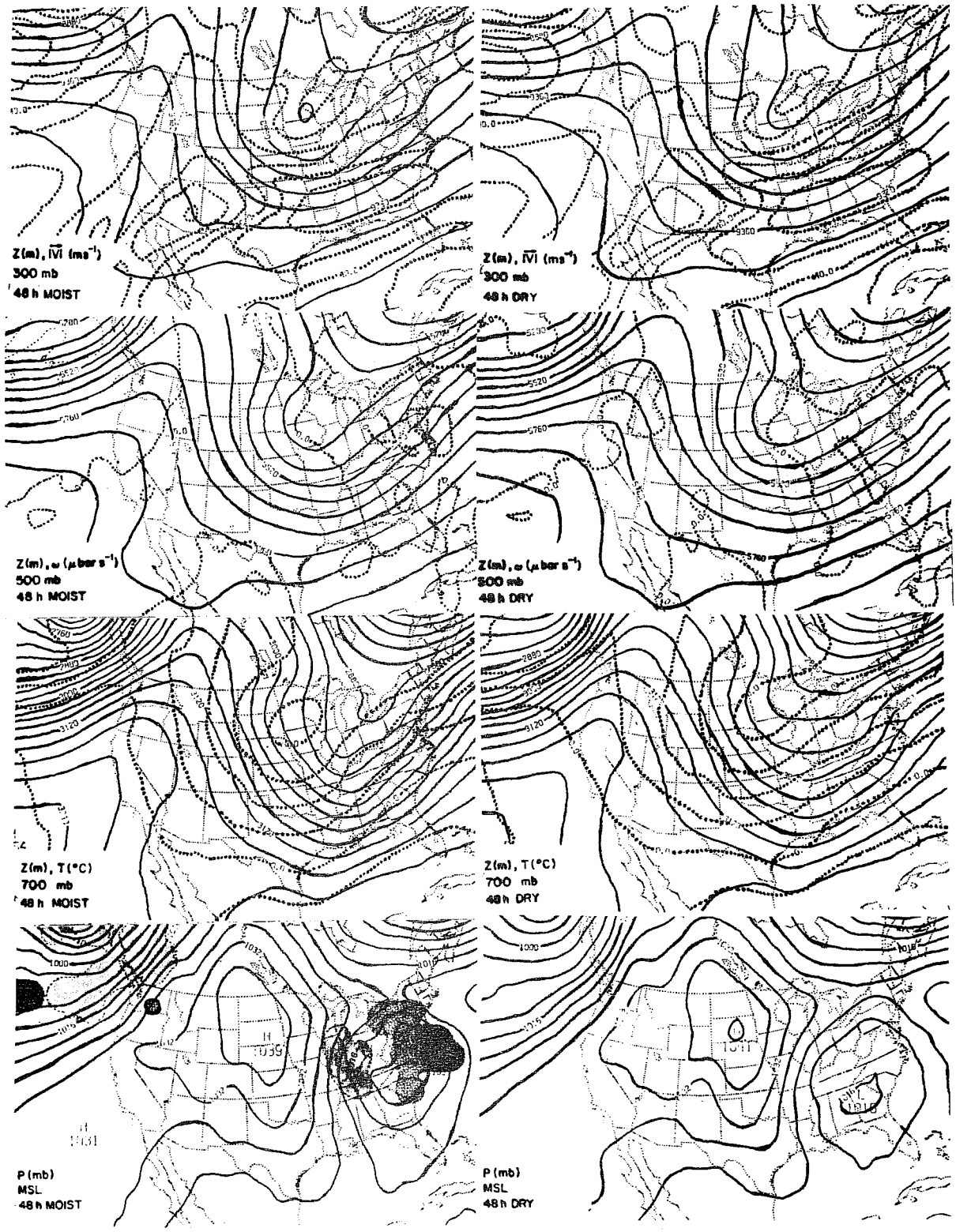

Fig. 9. As in Fig. 8 for 0000 GMT 9 January 1985 case.

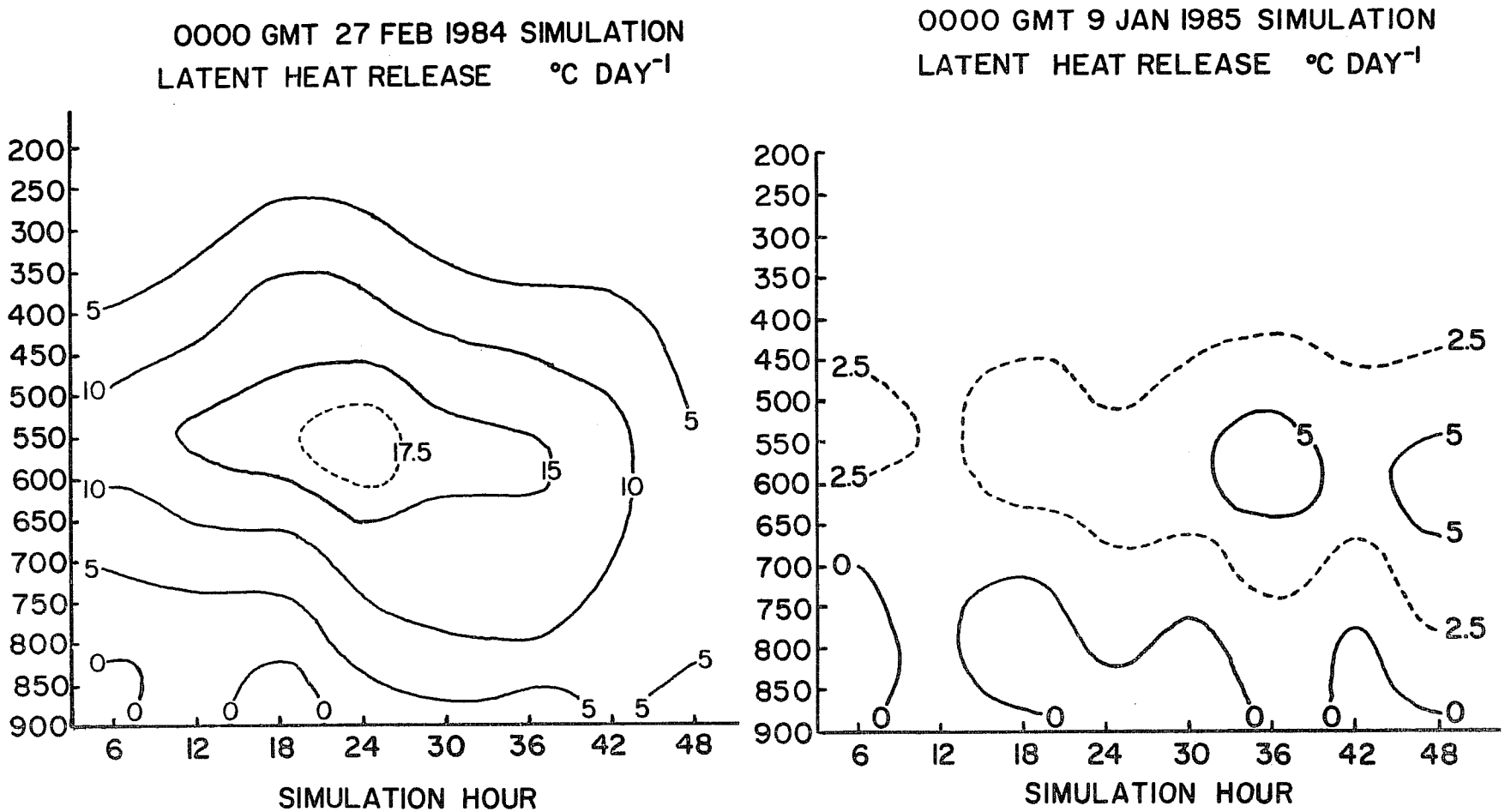

Fig. 10. Time/pressure cross-sections of cyclone-area average LHR for the two moist LFM simulations.

from the cyclone center, consistent with the cyclone's development and northeastward propagation. In contrast, term E forces height rises in the same region, thus acting to inhibit the development and propagation of the system, as discussed earlier. These conditions also prevail at higher levels (not shown), except that in terms B, C, and E the forcing is stronger and in term D height rises are found. The weaker January case is accompanied by weaker forcing, which for terms B and C also exhibits significantly different distributions. The term B height fall maximum is actually upstream from the cyclone center, while term C has a double maximum upstream and downstream from the cyclone center. The result is weaker forcing over the cyclone center, consistent with the lack of development of the system.

Comparisons of moist and dry simulated height tendencies are presented as cyclone average equivalent 6 h height changes at 700, 500, and 300 mb. Because such an area encompasses both height rises and falls, which tend to cancel in the averaging process, simple area averages are not adequate height tendency statistics. Since it is the magnitude of these rises and falls that is important, a suitable tendency statistic can be obtained by taking the average of the absolute value of the tendencies over the cyclone area.

Fig. 13 presents a comparison of mean absolute height changes forced by the sum of the four right-hand-side terms in (1). Clearly, the height changes are greater at higher levels, are two to three times larger in the February case, and are weaker in the dry forecast. In the February case, the net LHR influence is most pronounced at 700 mb but does extend to the other two levels. During the first 24 h, the mean absolute height change curves obtained from the moist and dry simulations diverge, reflecting the growing importance of latent heating over this period. However, over the last 24 h these two curves converge, reflecting a diminished importance for latent heating. In the January case, the moist and dry curves are significantly different only at 700 mb, confirming that the net LHR influence is confined to the lower troposphere. Also, in contrast to the February case, the two curves diverge over the last 24 h, reflecting a growing importance for latent heating throughout the 48 h period.

These distinctions between the moist and dry simulations are even more

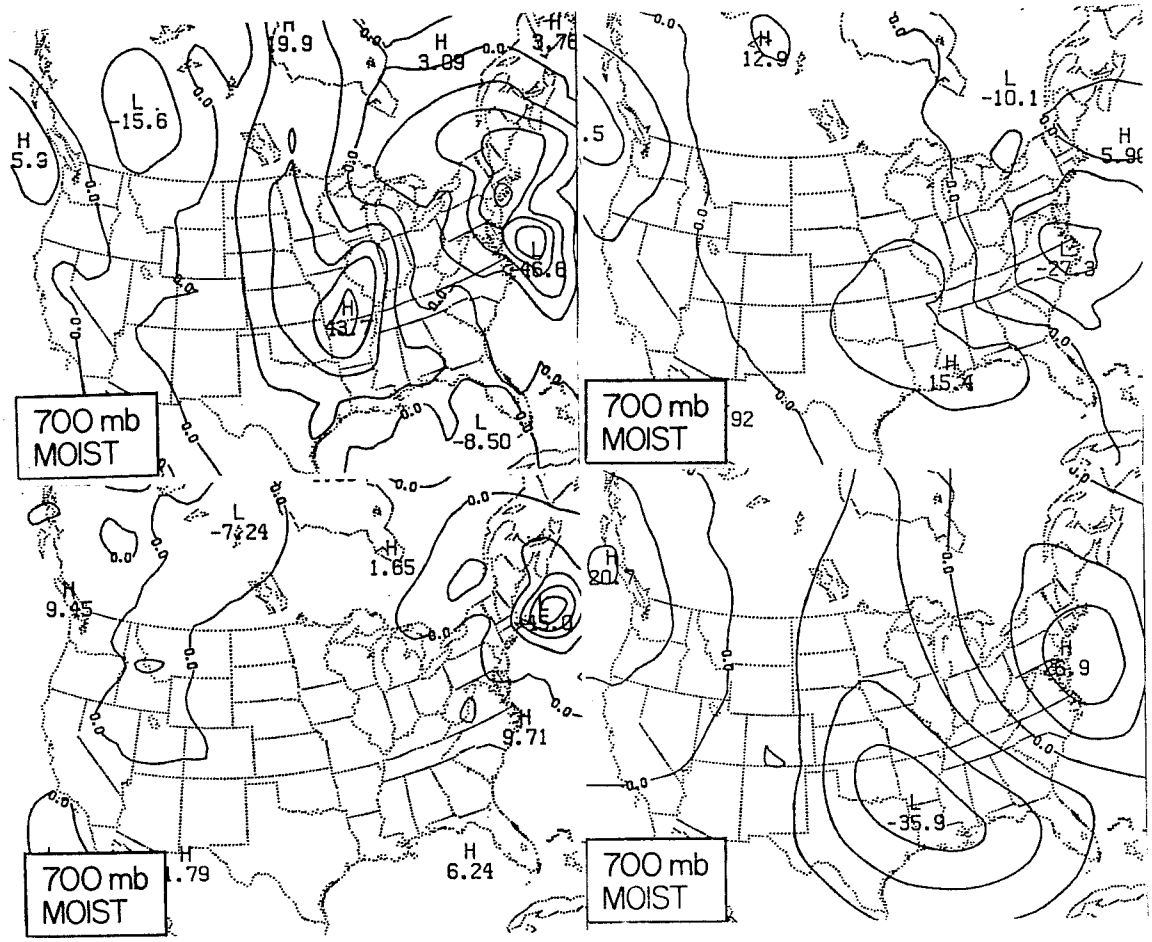

Fig. 11. 700 mb 6 h equivalent height change (m) for terms B (upper left), C (upper right), D (lower left), E (lower right) simulated by the moist model at 48 h for the February case.

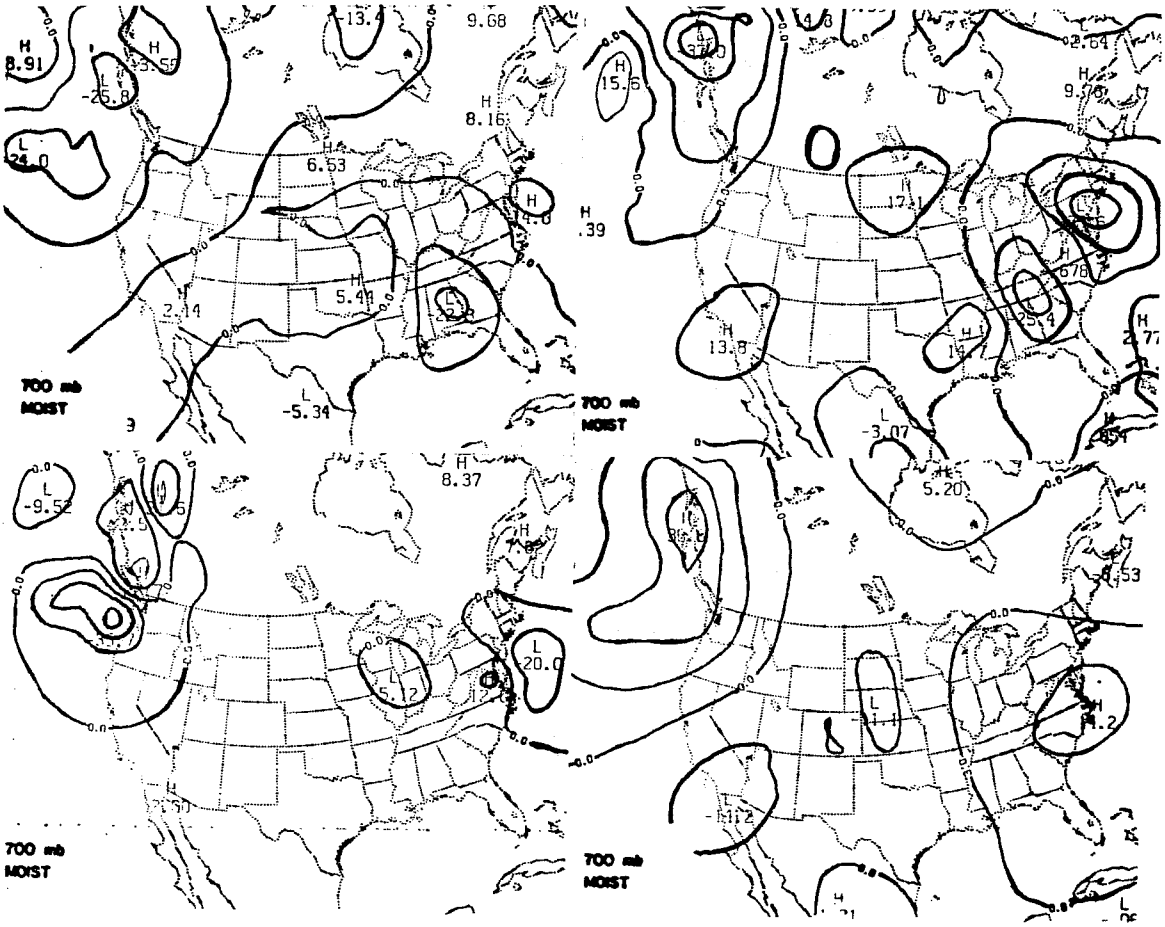

Fig. 12. As in Fig. 11 for the January case.

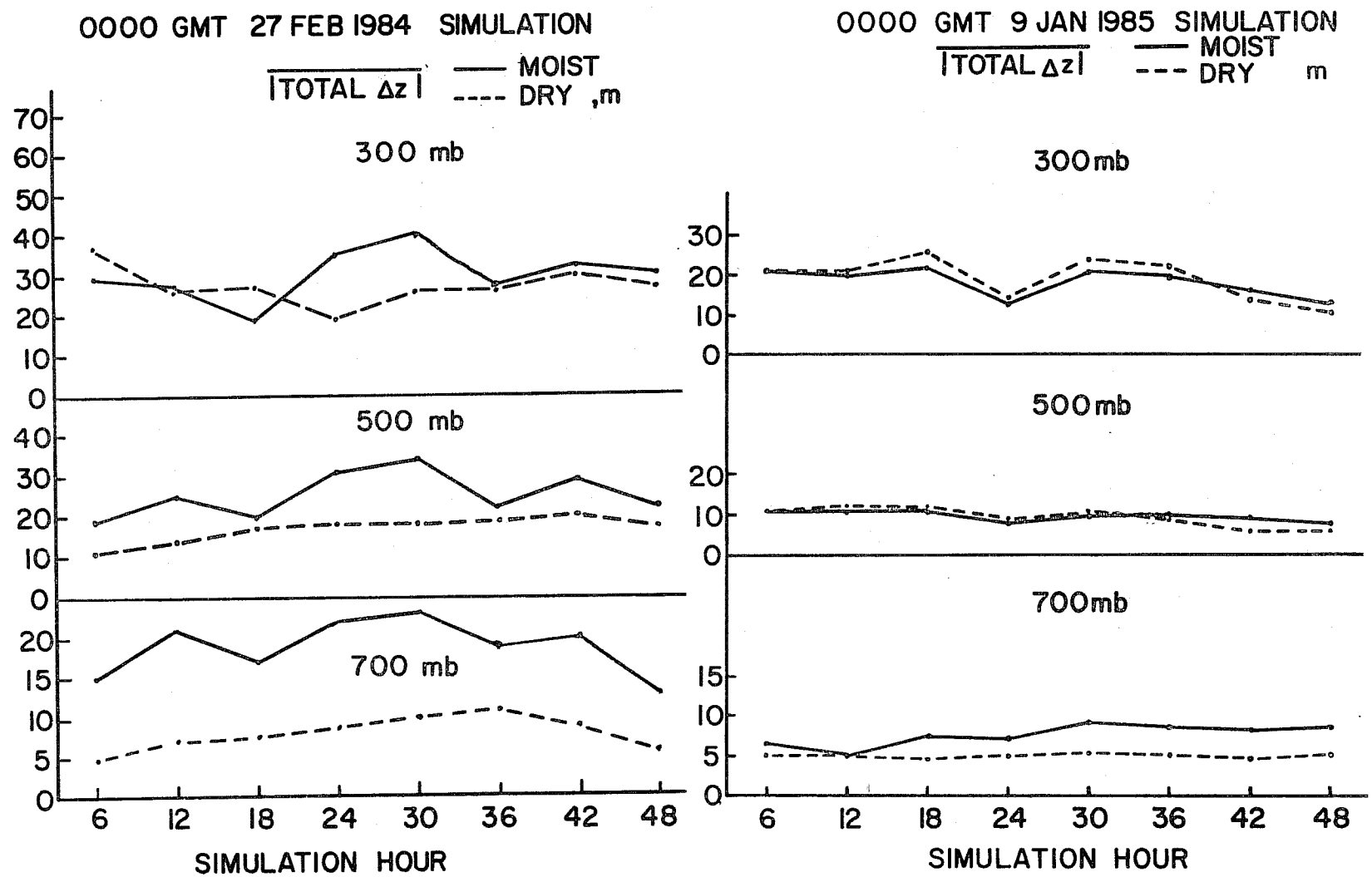

Fig. 13. Cyclone-area average absolute total height change (m) obtained from the moist and dry simulations for both cases.

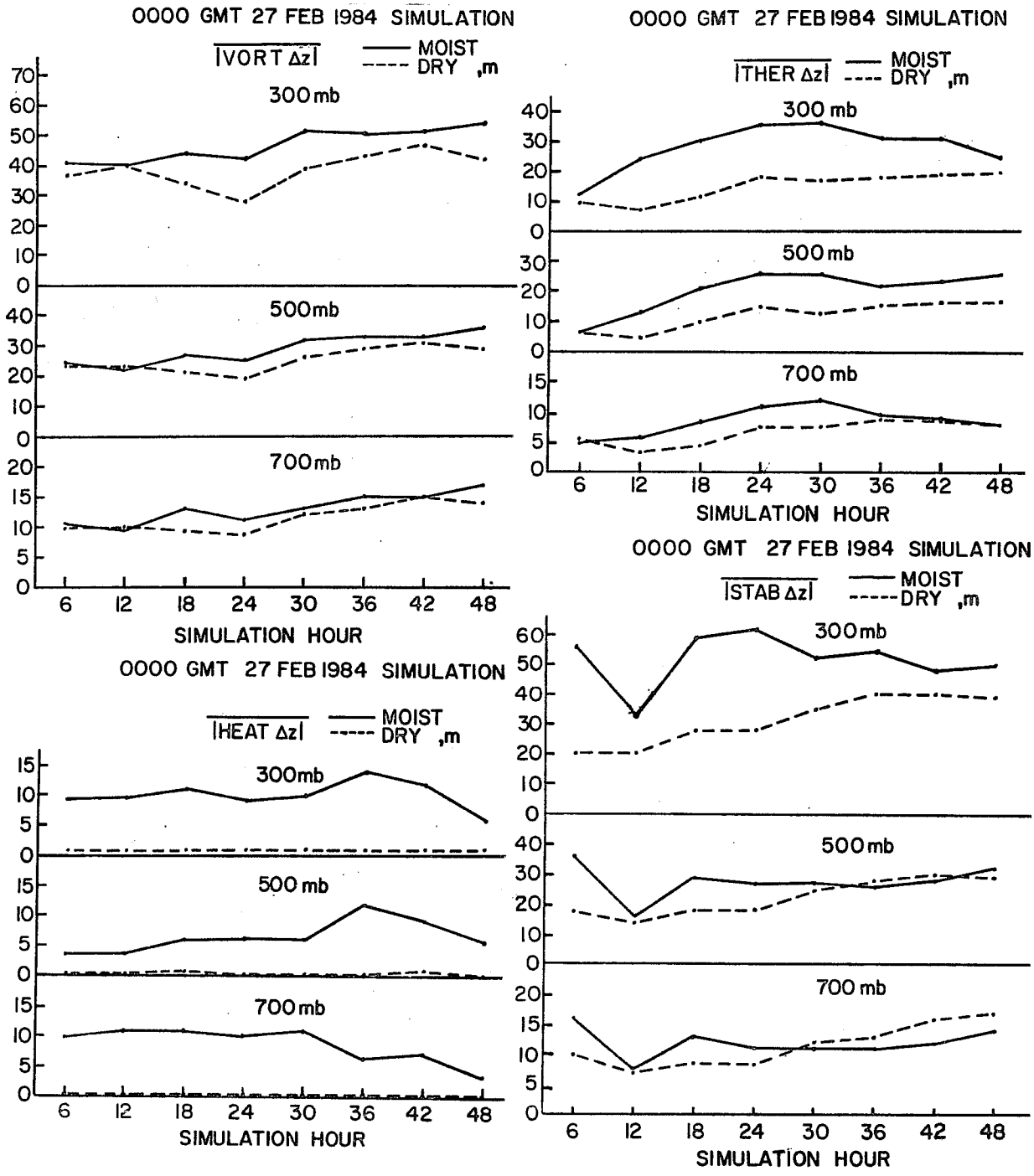

Fig. 14. As in Fig. 13 for the individual forcing terms simulated for the February case. Term B = VORT, C = THER, D = HEAT, E = STAB.

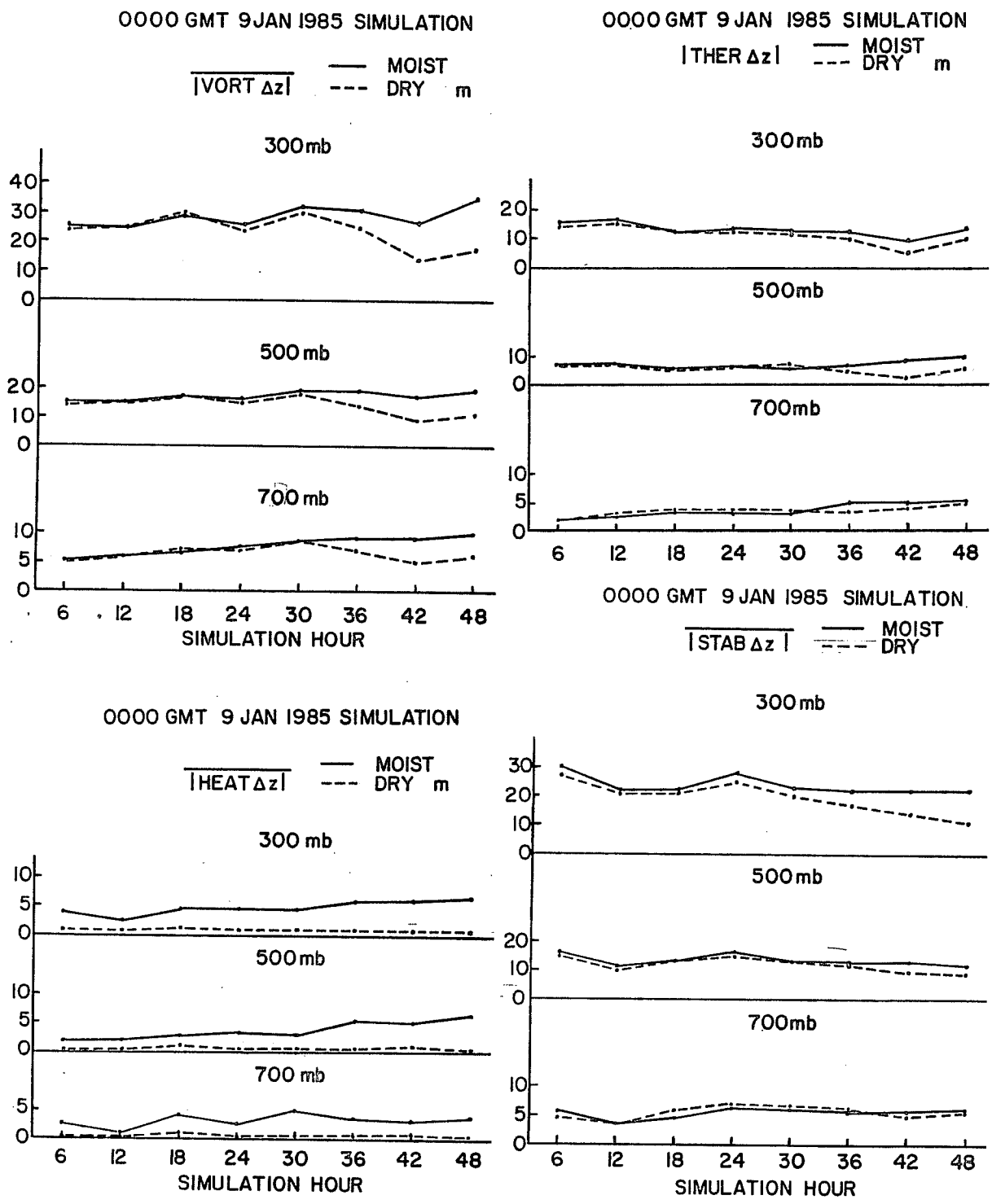

Fig. 15. As in Fig. 14 for the January case.

apparent in examinations of the mean absolute height changes forced individually by each of the right-hand-side terms in (1). Once again we see in the February case (Fig. 14) that the curves diverge during the first 24 h and converge during the last 24 h. Thus, the continued presence of latent heating during the last 24 h does not result in increasingly enhanced forcing in the moist simulation compared with the dry. In fact, at 700 mb the term B and C moist and dry forcing are nearly the same and the term E dry forcing is actually greater than the moist, by a sufficient amount to nearly offset the height falls associated with term D. As noted earlier, the moist surface cyclone develops during the first 24 h while the dry is decaying, and then both develop at a similar rate during the second 24 h. At 700 and 500 mb, the moist and dry simulated central heights diverge throughout the 48 h period; however, the rate of divergence decreases markedly after 24 h. The height tendency results suggest that this equilibration of the moist and dry development is reflected in a similar equilibration in all of the dynamic forcing terms. This response over the last 24 h is accompanied by two distinctive features of the latent heating field. First, as seen in Fig. 10, the heating decreases in magnitude, although marked decrease does not occur until the last 6 h; and second, the precipitation shield shifts to the east and north relative to the cyclone center.

In contrast, moist and dry height changes diagnosed for the January case (Fig. 15) are nearly the same for the first 24 h and then diverge over the second 24 h. This is consistent with the previously-noted differences in the cyclone development rates, the moist being nearly constant while the dry decays. In this case the latent heating maximizes at 36 h and then decreases slowly. However, the precipitation shield remains close to the cyclone center. The contrasting behavior of the two cases over the last 24 h and the correlation with the location of the latent heating field is consistent with Tracton's (1973) hypothesis that in some cases of extra-tropical cyclone development the release of latent heat in the vicinity of the cyclone center plays a crucial role.

Smith et al. (1984) hypothesize that LHR influences can be partitioned into "direct" and "indirect" components. In the context of this discussion, direct influences correspond to the impact of LHR on height changes through term D, while indirect influences are represented by the cumulative impact

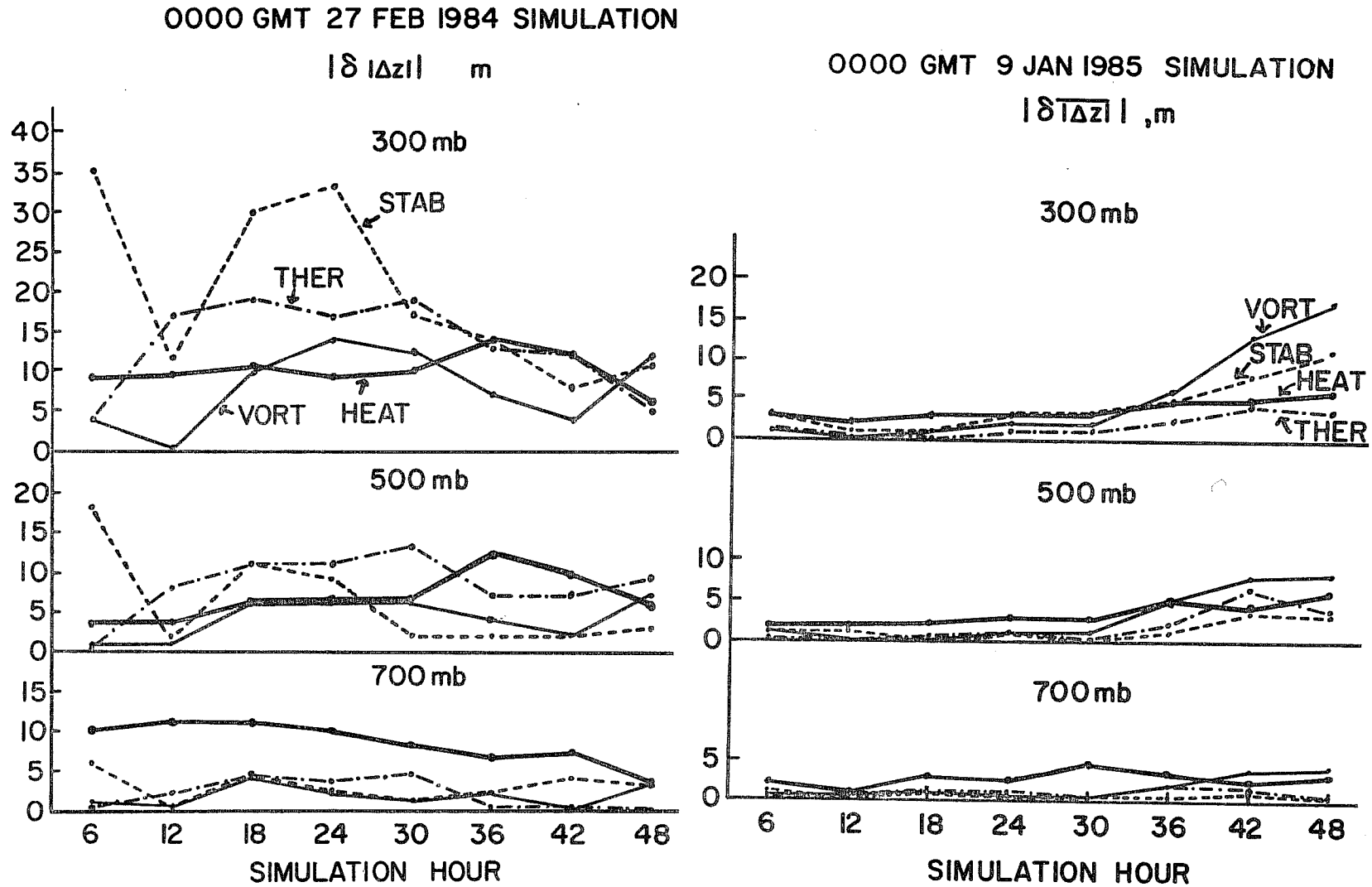

Fig. 16. Cyclone-area average absolute height change forced by term D and, for comparison, the average absolute differences between the moist and dry absolute height changes forced by terms B, C, E.

of LHR on terms B, C, and E. One of the results of the converging or diverging tendency curves in Figs. 14 and 15 is to change the relative importance of these direct and indirect influences. This is seen by comparing the cyclone-average absolute height changes forced by term D with absolute differences between the moist and dry height changes forced by terms B, C, and E. This comparison is presented for the two cases in Fig. 16. For the February case, it is quite apparent that the direct latent heating influence is dominant at 700 mb, but this diminishes with time. This direct influence is generally less than the indirect at 500 and 300 mb through the first 30 h. At these two levels the direct influence increases over the last 18 h while the indirect decreases, the latter a reflection of the converging moist and dry absolute height change curves. Thus, overall, the relative importance of the direct LHR influence grows as the cyclone matures. In the January case the direct influence dominates through the first 30 h, but then becomes relatively less important through the remainder of the simulation period. This last 18 h is marked by a decrease in the adiabatic forcing simulated by the dry model.

5. SUMMARY AND CONCLUSIONS

Using moist and dry numerical model simulations of ECY events, we conclude the following.

1) In cases of strong development, LHR is important but is not crucial for the development. However, in cases of weak development, the addition of LHR determines whether the cyclone will develop or decay.
2) For the two cases examined in detail, the net LHR influence extends to all levels in the more intense February case but is largely confined to the lower troposphere in the weak January case.
3) The similarity (dissimilarity) seen in the moist and dry development rates for the strong (weak) cyclone are also seen in moist and dry height changes forced by the three adiabatic forcing terms. These results are consistent with the changing position of the LHR shield relative to the cyclone center. The shield moves farther away from the cyclone center with time for the strong development case but remains near the cyclone center for the weak development case.
4) Both direct and indirect LHR influences are important in both cyclone cases, although the relative influence changes with time. The direct influence becomes relatively more (less) important with time in the strong (weak) development case.

ACKNOWLEDGEMENTS

I am pleased to acknowledge the significant contributions of three collaborators in this research, Dr. Patricia Pauley, Dr. David Smith, and Mr. John Zimmerman. I am also grateful to Dr. Dennis Deavon of NMC, who was so helpful during the implementation of the LFM; to Ms. Helen Henry for typing the manuscript; and to Mr. Richard Knabb for drafting the figures. This paper is based upon work supported by the National Science Foundation under Grant Nos. ATM 821942 and ATM 8508941.

REFERENCES

Anthes, R.A., and D. Keyser, 1979: Test of a fine-mesh model over Europe and United States. Mon. Wea. Rev., 107, 963-984.

_____, Y.H. Kuo, S.G. Benjamin, and Y.F. Li, 1982: The evolution of the mesoscale environment of severe local storms: Preliminary modeling results. Mon. Wea. Rev., 110, 1187-1213.

Aubert, E.J., 1957: On the release of latent heat as a factor in large scale atmospheric motions. J. Meteor., 14, 527-542.

Bosart, L.F., 1981: The Presidents' Day snowstorm of 18-19 February 1979: A subsynoptic-scale event. Mon. Wea. Rev., 109, 1542-1566.

Bullock, B.R., and D.R. Johnson, 1971: The generation of available potential energy by latent heat release in a midlatitude cyclone. Mon. Wea. Rev., 99, 1-14.

Chang, C.B., D.J. Perkey, and C.W. Kreitzberg, 1981: A numerical case study of the squall line of 6 May 1975. J. Atmos. Sci., 38, 1601-1615.

_____, _____, and _____, 1982: A numerical case study of the effects of latent heating on a developing wave cyclone. J. Atmos. Sci., 39, 1555-1570.

_____, _____, and _____, 1984: Latent heat induced transformations during cyclogenesis. Mon. Wea. Rev., 112, 357-367.

Chen, T.C., C.B. Chang, and D.J. Perkey, 1983: Numerical study of an AMTEX '75 oceanic cyclone. Mon. Wea. Rev., 111, 1818-1829.

Danard, M.B., 1964: On the influence of released latent heat on cyclone development. J. Appl. Meteor., 3, 27-37.

_____, 1966a: A quasi-geostrophic numerical model incorporating effects of release of latent heat. J. Appl. Meteor., 5, 85-93.

_____, 1966b: On the contribution of released latent heat to changes in available potential energy. J. Appl. Meteor., 5, 81-84.

Dare, P.M., and P.J. Smith, 1984: A comparison of observed and model energy balance for an extratropical cyclone system. Mon. Wea. Rev., 112, 1289-1308.

DiMego, G.J., and L.F. Bosart, 1982: The transformation of tropical storm Agnes into an extratropical cyclone. Part I: The observed fields and vertical motion computation. Mon. Wea. Rev., 110, 385-411.

Gerrity, J.P., 1977: The LFM model--1976: A documentation. NOAA Technical Memorandum NWS NMC 60. National Meteorological Center, World Weather Building, Washington, DC 20233.

Gyakum, J.R., 1983a: On the evolution of the QEII Storm. Part I: Synoptic aspects. Mon. Wea. Rev., 111, 1137-1155.

_____, 1983b: On the evolution of the QEII Storm. Part II: Dynamic and thermodynamic structure. Mon. Wea. Rev., 111, 1156-1173.

Holton, J.R., 1979: An Introduction to Dynamic Meteorology, 2nd ed., Academic Press, 391 pp.

Kenney, S.E., and P.J. Smith, 1983: On the release of eddy available potential energy in an extratropical cyclone system. Mon. Wea. Rev., 111, 745-755.

Keyser, D.A., and D.R. Johnson, 1984: Effects of diabatic heating on the ageostrophic circulation of an upper tropospheric jet streak. Mon. Wea. Rev., 112, 1709-1724.

Krishnamurti, T.N., 1968: A study of a developing wave cyclone. Mon. Wea. Rev., 96, 208-217.

Lin, S.C., and P.J. Smith, 1979: Diabatic heating and generation of available potential energy in a tornado-producing extratropical cyclone. Mon. Wea. Rev., 107, 1169-1183.

_____, and _____, 1982: The available potential energy budget of a severe storm-producing extratropical cyclone. Mon. Wea. Rev., 110, 522-533.

Newell, J.E., and D.G. Deaven, 1981: The LFM-II model--1980. NOAA Technical Memorandum NWS NMC 66. National Meteorological Center, World Weather Building, Washington, DC 20233.

Pagnotti, V., and L.F. Bosart, 1984: Comparative diagnostic case study of east coast secondary cyclogenesis under weak versus strong synoptic-scale forcing. Mon. Wea. Rev., 112, 5-30.

Perkey, D.J., 1976: a description and preliminary results from a model for forecasting quantitative precipitation. Mon. Wea. Rev., 104, 1513-1526.

_____, and C.W. Kreitzberg, 1976: A time-dependent lateral boundary scheme for limited-area primitive equation models. Mon. Wea. Rev., 104, 744-755.

Reed, R.J., and M.D. Albright, 1986: A case study of explosive cyclogenesis in the eastern Pacific. Mon. Wea. Rev., 114, 2297-2319.

Robertson, F.R., and P.J. Smith, 1983: The impact of model moist processes on the energetics of extratropical cyclones. Mon. Wea. Rev., 111, 723-744.

Smith, P.J., P.M. Dare, and S.J. Lin, 1984: The impact of latent heat release on synoptic-scale vertical motions and the development of an extra-tropical cyclone system. Mon. Wea. Rev., 112, 2421-2430.

_____, and _____, 1986: The kinetic and available potential energy budget of a winter extratropical cyclone system. Tellus, 38A, 49-59.

Tracton, M.S., 1973: The role of cumulus convection in the development of extratropical cyclones. Mon. Wea. Rev., 101, 573-593.

Tsou, C.-H., P.J. Smith, and P.M. Pauley, 1987: A comparison of adiabatic and diabatic forcing in an intense extratropical cyclone system. Mon. Wea. Rev., 115, 763-786.

Vincent, D.G., G.B. Pant, and H.J. Edmon, Jr., 1977: Generation of available potential energy of an extratropical cyclone system. Mon. Wea. Rev., 105, 1252-1265.